8

Single Neurons and the Perception of Visual Motion

William T. Newsome
Department of Neurobiology
Stanford University Medical School
Stanford, CA 94305

Kenneth H. Britten
Department of Neurobiology
Stanford University School of Medicine

J. Anthony Movshon
Department of Psychology
Center for Neural Science
New York University
New York, NY

Michael Shadlen
Department of Neurobiology
Stanford University School of Medicine

The middle temporal area (MT) of primates is a cortical visual area that plays a prominent role in the analysis of visual motion. We have examined the relationship between the responses of MT neurons and motion perception by conducting electrophysiological recordings as a rhesus monkey performed a direction discrimination task near the limits of performance. Using a signal detection analysis of the neuronal responses, we found that the sensitivity of many MT neurons to the motion signals in our stimuli equaled or exceeded the monkey's psychophysical sensitivity. For some neurons, we also observed a trial-by-trial relationship between the intensity of the neuron's response and the perceptual judgment made by the monkey. When considered together with a previous lesion study, these results suggest that perceptual decisions in this task are based in a relatively direct manner on the directional information encoded by MT neurons.

Introduction

In primates, visual perceptual decisions are based predominantly on the responses of cortical neurons to visual stimuli. The exact nature of this relationship is, however, far from clear. The visual cortex of primates comprises a large number of visual areas organized in a complex hierarchy that incorporates both serial and parallel principles.[1,2] Thus any particular visual stimulus will presumably influence the responses of a formidable number of neurons in widely disparate areas of the visual cortex. However, some perceptual decisions, such as those made by an observer working near the limits of performance, may depend upon the responses of a small subset of the neurons activated by the visual stimulus. For example, judgments concerning the direction of motion of a visual pattern appear to depend on directionally selective neurons of the visual cortex[3-5] even though such neurons constitute a modest fraction of the total activated by the pattern. If the moving pattern is spatially complex such that its direction of motion must be computed from several component motion vectors, the psychophysical judgment may hinge upon a yet smaller subset of directionally selective cortical neurons.[6] Thus the neurons that provide the critical signals for a perceptual decision may be both few in number and well localized within the visual system despite the large and distributed nature of the complete population of neurons responding to the stimulus.

Ideally, a physiological understanding of such a perceptual process would include: (1) identification of the neurons that provide the critical signals for the perceptual decision, (2) insight into the way these signals arise from the inputs provided by lower centers, and (3) knowledge of the mechanisms by which the critical signals are translated into a decision. We are addressing these issues by recording the responses of cortical neurons in alert rhesus monkeys trained on a perceptual task requiring a visual discrimination of direction of motion. In a previous lesion study, Newsome and Paré[5] found that the middle temporal visual area (MT), an extrastriate area near the junction of the occipital, parietal and temporal lobes, is necessary for normal performance on a direction discrimination task. This observation is consistent with physiological data obtained in anesthetized monkeys, since 80-90 percent of the neurons in MT encode motion information in the form of direction and speed selective responses.[7-10] Additional anatomical and physiological studies have described an extended pathway, including MT, that appears to process motion information relevant to a number of behavioral tasks.[2] It thus appears possible to investigate the neuronal basis of perceptual decisions involving direction discrimination by recording at several loci on this pathway in trained animals. We have now recorded the responses of MT neurons while simultaneously measuring the monkey's psychophysical thresholds for direction discrimination. We have found that many MT neurons are sufficiently sensitive to the motion signals to form the basis for the monkey's psychophysical performance, and we have observed a trial-to-trial association between the strength of neuronal responses and the perceptual decision made by the monkey. These MT neurons could provide the critical signals used by the monkey to make perceptual decisions in this task.

The Paradigm

The visual stimuli we employ are dynamic random dot patterns in which a specifiable proportion of the dots pro-

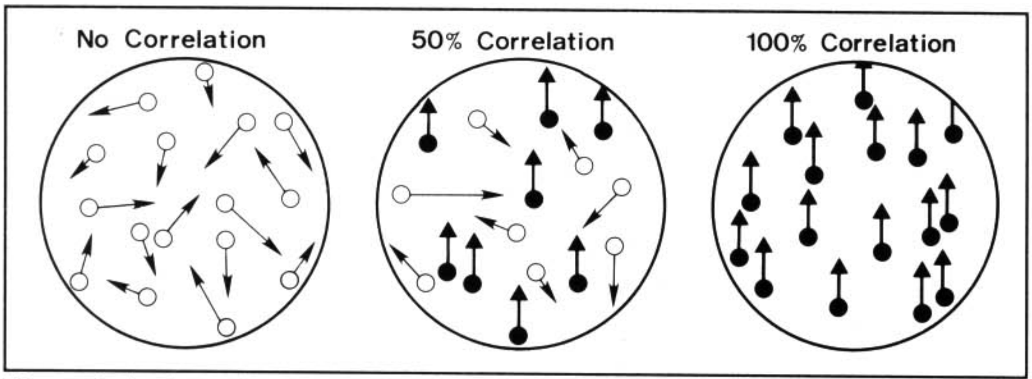

Figure 1. A schematic representation of the dynamic random dot stimuli employed in these experiments. Each stimulus was formed by plotting dots in rapid succession on the face of an *X-Y* oscilloscope using a high speed D-to-A converter. Each dot survived for a brief period of time before being replaced. In the 0 percent correlation case on the left, the replacement dots were plotted at random locations on the screen so that the dot field appeared as twinkling visual noise with no correlated motion in any single direction. In the 100 percent correlation state on the right, each dot was replaced by a partner with a constant offset in space and time. In this state, the display took the form of a conventional random dot pattern in which the motion of each dot was identical to the correlated motion of the entire display. In intermediate states such as that for 50 percent correlation (middle), a specifiable percentage of the dots carried the correlated motion signal while the remaining dots provided dynamic masking noise. A two-alternative, forced-choice procedure was used to determine the threshold correlation for which monkeys could successfully discriminate opposed directions of motion. Reprinted with permission from reference 5.

vides a correlated motion signal that is spatially dispersed among masking motion noise. At one extreme of the stimulus range, illustrated in the left-hand panel of Figure 1, dots are plotted successively at random locations on the screen, survive for a short period of time, and are replaced by dots at other randomly selected locations. The overall visual effect is one of twinkling noise similar to that seen on a television tuned between stations. In this state, which we refer to as zero percent correlation, there are many local motion events that result from fortuitous pairings between successively plotted dots (arrows), but there is no net, or correlated, motion in any single direction. At the other extreme, illustrated in the right-hand panel of Figure 1, each dot that disappears is replaced by a partner dot with a constant offset in space and time. This state, which we refer to as 100 percent correlation, corresponds to a conventional random dot pattern in which the motion of each dot is identical to the net motion of the entire pattern. In most trials, the monkey actually viewed an intermediate display such as that illustrated in the middle panel of Figure 1. In this state, a portion of the dots carried a correlated motion signal while the rest provided random motion noise. As described previously by Newsome and Paré,[5] we used a two-alternative, forced-choice psychophysical procedure to measure the threshold correlation for which the monkeys could successfully discriminate opposed directions of motion in these displays.

Our procedure for obtaining simultaneously physiological and psychophysical data is illustrated in Figure 2. Initially, we isolated an MT neuron,

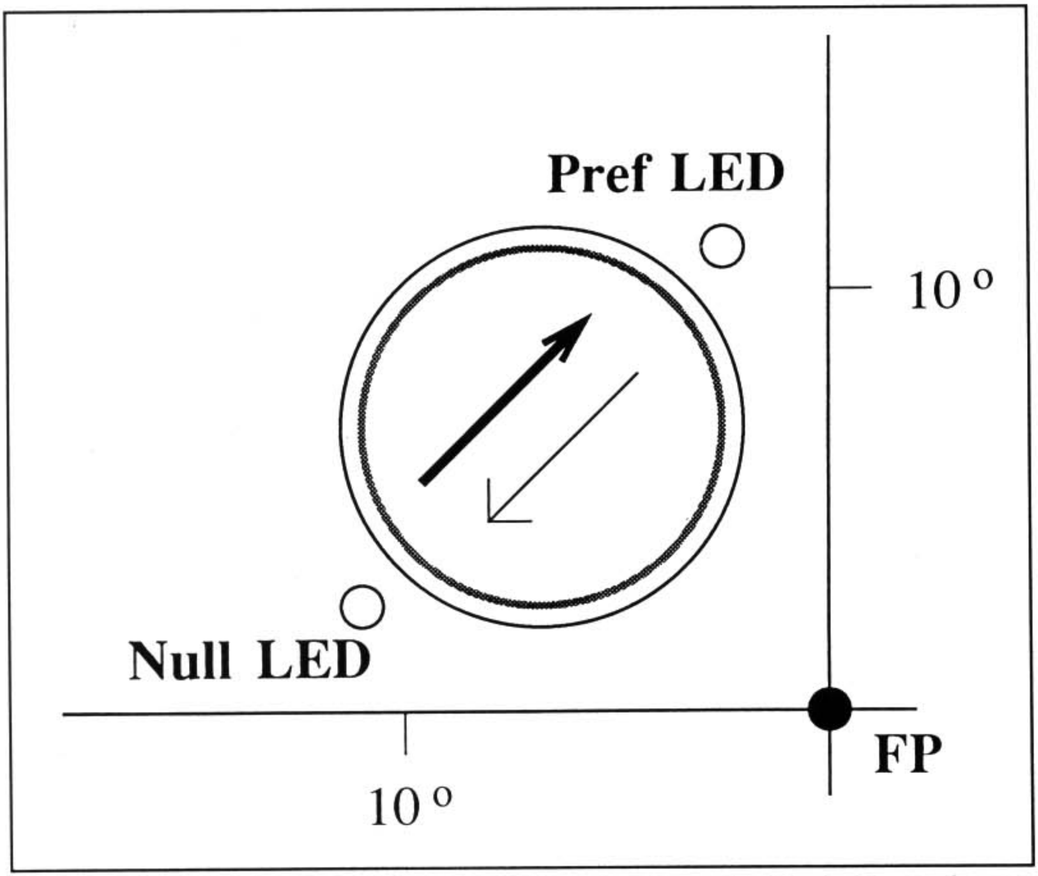

Figure 2. Experimental paradigm for obtaining psychophysical and physiological data on the same set of trials. The receptive field of a directionally selective neuron was mapped (thick circle) while the monkey maintained his gaze on a centrally located fixation point (FP). The preferred (thick arrow) and null (thin arrow) directions and optimal speed were identified qualitatively. The monkey then performed direction discriminations on a series of trials in which the correlated motion signal appeared in either the preferred or null direction of the neuron. The speed of the dots in correlated motion was matched to the preferred speed of the neuron, and the dots appeared within an aperture (thin circle) that just covered the receptive field of the neuron. The monkey held its gaze on the fixation point for a two second interval while the random dot stimulus appeared within the aperture. At the end of the two second viewing interval, the fixation point was extinguished and two target LED's appeared which corresponded to the preferred (Pref LED) and null (Null LED) directions of motion. The monkey reported its judgement of the direction of correlated motion by transferring its gaze to the corresponding LED target. By noting the monkey's performance on a number of trials (at least 30) at each of several correlation levels, we measured the psychophysical threshold while simultaneously recording the responses of the cortical neuron.

mapped its receptive field (thick circle), and identified its preferred direction of motion (thick arrow). We considered the null direction (thin arrow) to be 180 degrees opposed to the preferred direction. We then placed the aperture containing the random dot pattern (thin circle) directly over the neuron's receptive field, and we matched the size of the aperture to the size of the receptive field. In addition, we set the speed of the moving dots to be near the optimal speed for the cell. We then presented a block of trials in which the strength and the direction of the correlated motion signal varied from trial to trial. A range of correlation levels was chosen to span the psychophysical threshold, and an equal number of trials was presented at each correlation level: half in the neuron's preferred direction and half in the null direction. The monkey obtained a liquid reward for correctly reporting the direction of motion in each trial. By tailoring the parameters of the random dot stimulus (aperture location and size, speed, and axis of motion) to be optimal for each neuron recorded, we sought to maximize the chance that the observed neuronal responses would contribute to the monkey's perceptual decisions.

In each trial of the threshold measurement, the monkey directed its gaze toward a fixation point (FP) directly in front of him. The random dot stimulus then appeared for two seconds within the neuron's receptive field, after which the fixation point and the random dot pattern disappeared. As the fixation point was extinguished, two target LED's appeared, one corresponding to the neuron's preferred direction (Pref LED) and the other to the neuron's null direction (Null LED). The monkey then indicated its decision concerning the direction of stimulus motion by making a saccadic eye movement to one of the two target LED's.

We measured the monkey's eye position throughout each trial using the scleral search coil technique. If the monkey broke fixation during the stimulus presentation period, we aborted the trial and discarded the data. In this manner we ensured that the random dot pattern remained within the neuron's receptive field for the entire two second viewing interval.

We compiled the psychophysical data into psychometric functions like the one shown in Figure 3; the proportion of correct responses is plotted against the strength of the motion signal. Typically, as in the case shown in Figure 3, choice performance was perfect for strong motion signals and fell to near chance for weak ones. We used a maximum-likelihood method[11] to fit these data with functions of the form

$$p = 1 - (1 - \gamma) \exp[-(c/\alpha)^{\beta}] \tag{1}$$

where C is stimulus correlation, γ is the "guessing" probability (that is, the probability of getting a correct choice by chance, in our case 0.5), α is the correlation level supporting "threshold" performance (in our case threshold performance is considered to be 0.82, or 82 percent correct) , and β is a parameter governing the slope of the function. This function is the integral of the Weibull distribution and was introduced to psychophysics in this form by Quick.[12] We found that it provided a good fit to most of our data, better, for example, than the Gaussian integrals or other plausible forms for the psychometric function. For the case shown in Figure 3, the threshold (α) was 0.062 (6.2 percent correlation), and the slope of the function (β) was 0.88.

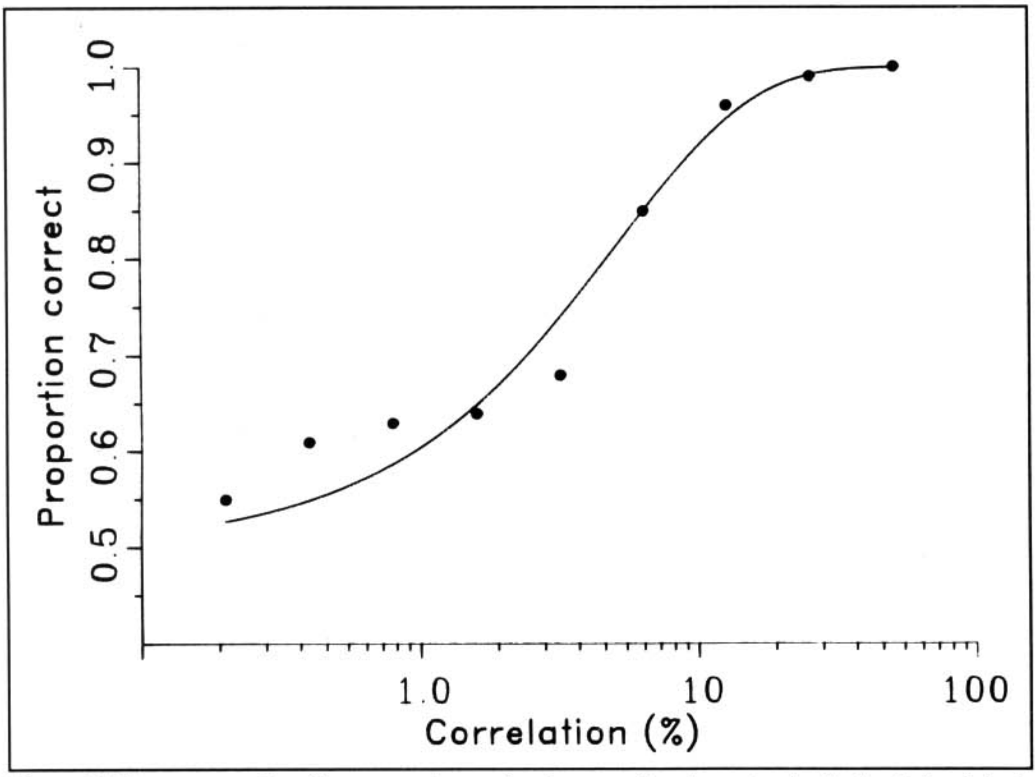

Figure 3. The perceptual performance of a monkey in a combined psychophysical and physiological experiment. The abscissa shows the percentage of dots in correlated motion. High correlations indicate strong motion signals; low correlations represent weak signals. The ordinate depicts the proportion of trials on which the monkey correctly reported the direction of motion of the correlated signal. 120 trials were presented at each correlation, half in the preferred direction and half in the null direction. The monkey performed flawlessly at the highest correlation, but its performance was random (near 50 percent correct) at the lowest correlation. The data points were fitted with a sigmoidal curve as described in the text. Threshold was taken to be the correlation level that corresponded to 82 percent correct performance. For the data illustrated here, threshold was 6.22 percent correlation.

Comparison of Neuronal and of Psychophysical Sensitivities

Figure 4 shows the physiological data that we obtained during the psychophysical threshold measurement illustrated in Figure 3. The circles connected by the solid line indicate the neuron's responses to stimulus motion in the preferred direction for each of eight correlation levels; the squares connected by the dashed line depict the neuron's response to null direction motion. The neuron exhibited typical direction-selective behavior at high correlation levels: it responded vigorously to motion in its preferred direction, but was relatively unaffected by motion in its null direction (the spontaneous discharge rate is indicated by the triangle). As the correlation level decreased, however, the neuron became steadily less sensitive to directional differences in the motion of the dot pattern.

This effect can be seen more clearly

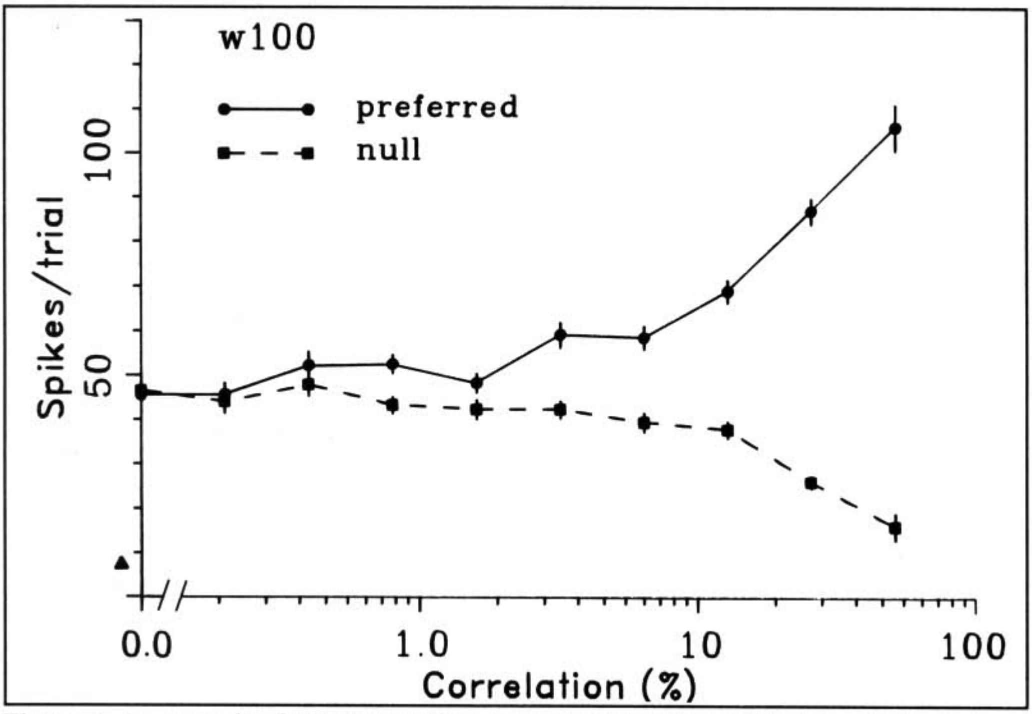

Figure 4. An example of the physiological data recorded in a combined psychophysical and physiological experiment. The abscissa shows the percentage of dots in correlated motion, and the ordinate indicates the response of the neuron (number of action potentials recorded during the two second viewing interval). Each symbol represents the mean of the responses on 60 trials; the error bars indicate standard errors of the means. The responses shown by the circles and solid line are for preferred direction trials; the responses indicated by the squares and dashed line are for null direction trials. For high correlations, the neuron was strongly direction selective, but low correlations yielded statistically indistinguishable responses for the two directions of motion. The triangle at the lower left depicts the spontaneous firing rate for this cell. We observed a range of responses to stimuli with zero percent correlation; many neurons, like this one, responded well while others responded poorly or not at all.

in the histograms of Figure 5A. The three pairs of histograms show the complete distributions of spike counts elicited by preferred (hatched bars) and null (solid bars) direction motion for three of the correlation levels depicted in Figure 4. The distributions were virtually nonoverlapping at 25.6 percent correlation, but were essentially the same at 0.4 percent correlation. As the correlation level moved between these two values, the neuron underwent a transition that was qualitatively similar to that seen in the monkey's behavior in Figure 3: the neuron provided a reliable basis for directional discrimination at large correlation values, it failed to do so at low correlation values.

In order to compare quantitatively the performance of the neuron on a discrimination task to that of the monkey, we employed a simple discrimination model in which the perceptual decision for each trial is based on a comparison of the responses of two oppositely tuned directional neurons such as those illustrated in Figure 6 (the receptive fields of the two neurons would be superim-

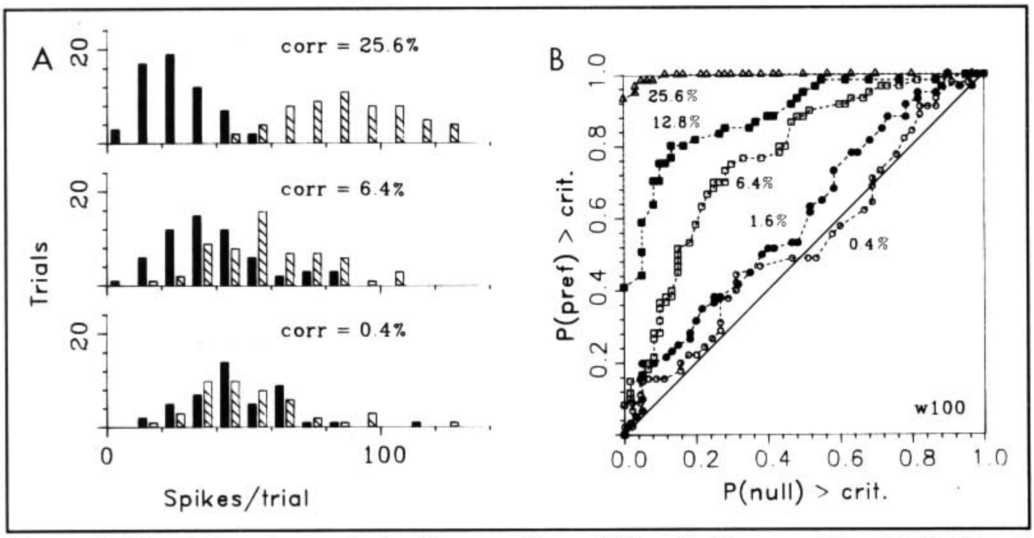

Figure 5. Signal detection analysis of neuronal sensitivity. **A.** The complete distribution of responses obtained for stimulus motion in the preferred (hatched bars) and null (solid bars) directions for three of the correlation levels illustrated in Figure 4. The abscissa shows the response in spikes per trial; the ordinate indicates the number of trials for which each response was observed. The response distributions for preferred and null directions overlap very little at 25.6 percent correlation, but are statistically indistinguishable at 0.4 percent correlation. **B.** Receiver operating characteristics (ROC curves) for five selected correlation levels, including the three illustrated in A. An ROC curve is generated by plotting, for each possible criterion level, the proportion of responses in the "null" distribution (solid bars) that exceed criterion against the proportion of responses in the "preferred" distribution (hatched bars) that exceed criterion. These proportions are first calculated for a criterion level of one spike per trial, in which case the point falls at the top right corner of the unit square. The proportions are then calculated and plotted for successively higher criterion levels until no responses in either distribution exceed criterion, in which case the point falls at the lower left corner of the unit square. The resulting ROC curve provides a description of the sensitivity of the neuron to the directional signals at that correlation level. The area under the ROC curve represents the performance level that would result from strict adherence to the decision rule in Figure 5. At 0.4 percent correlation, the proportion of the unit square that falls below the ROC curve is 0.535, corresponding to near random performance (53.5 percent correct). At 25.6 percent correlation, the area below the ROC curve is 0.997, corresponding to nearly perfect performance (99.7 percent correct).

posed in space, but are separated in the figure for clarity). In a given trial, motion will be judged as rightward if the "neuron" in Figure 6 responds more strongly than the "antineuron." If the "antineuron" responds more strongly, motion will be judged as leftward. (Psychophysical studies of direction-specific adaptation and the motion aftereffect support the notion that directional judgments are based on the relative responses of oppositely tuned directional mechanisms.[13,14])

We have obtained two of the three types of data needed to evaluate the performance of this model; we know the monkey's psychophysical responses and the responses of the "neuron" on each trial, but we do not know the responses of the "antineuron." To circumvent this difficulty, we assumed that the response distributions of the

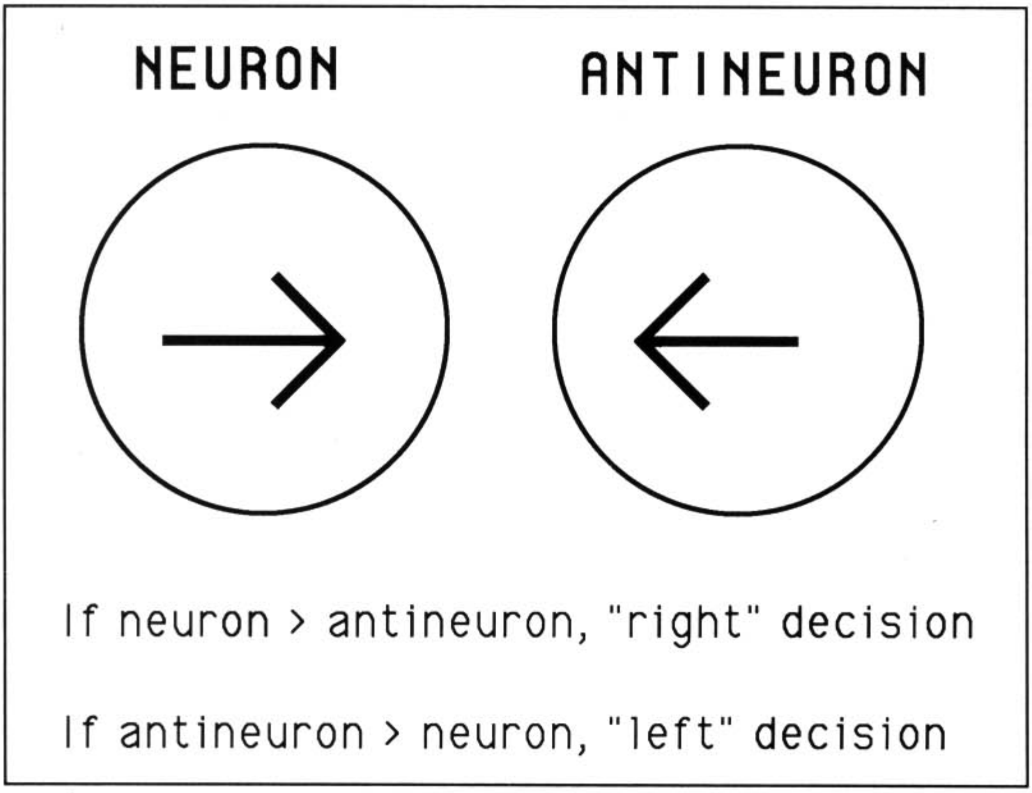

Figure 6. A simple model for evaluating the discrimination performance of an MT neuron. In the model, discrimination of oppositely directed motion signals is accomplished by comparing the responses of two directionally selective neurons whose preferred directions are opposed. In the example, motion can be rightward or leftward on a given trial. The response of the "neuron," which prefers rightward motion, is compared to that of the "antineuron," which prefers leftward motion. If the response of the "neuron" is larger on a given trial, the direction of motion will be judged as rightward. If the "antineuron" generates a larger response, motion will be judged as leftward. The receptive fields of the two neurons would be coextensive so that they respond to stimuli over equivalent regions of visual space. In the figure, however, the receptive fields are displaced from each other for clarity.

antineuron are identical to those of the neuron with the sole modification that its preferred direction is opposite to that of the neuron. Under this assumption, the histograms illustrated in Figure 5 can represent the responses of both the neuron and the antineuron, with the preferred direction being reversed for the antineuron. Thus the decision on a given trial will be based on the comparison of a response selected from a hatched distribution in Figure 5 with a response selected from the accompanying solid distribution. For stimulus motion to the right, the hatched distribution will correspond to the responses of the "neuron" (preferred direction rightward) and the solid distribution will represent the responses of the "antineuron" (null direction rightward); for leftward motion, the opposite relation will obtain. If there is no correlation in the activity of "neuron" and "antineuron," the responses compared

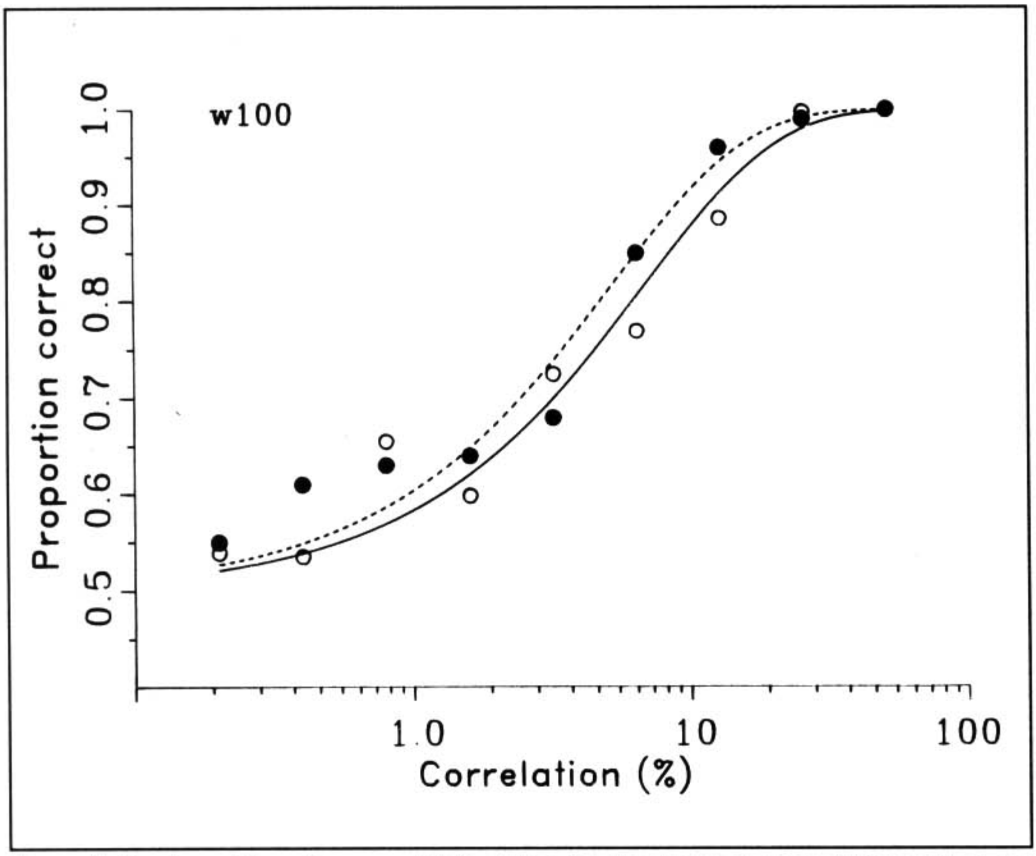

Figure 7. Psychometric and neurometric functions for simultaneously recorded perceptual and physiological data. The solid circles and dashed line are the same psychophysical data illustrated in Figure 3. The open circles and solid line indicate the performance of the MT neuron as derived from a signal detection analysis of neuronal responses (see text). Perceptual threshold for the monkey was 6.22 percent correlation; threshold for the neuron was 6.87 percent correlation.

on a given trial will be drawn randomly from the two distributions.

We used a method based on signal detection theory[15] to compute expected discrimination performance given the data illustrated in Figures 4 and 5 and the decision rule outlined in Figure 6.[16] For each correlation level tested, we computed an ROC (receiver operating characteristic) by plotting, for a series of criterion response levels, the proportion of preferred direction trials that exceeded criterion against the proportion of null direction trials that exceeded criterion. Consider, for example, the response distributions for the zero percent correlation trials (lower panel, Figure 5A). For a low criterion level, such as 5 spikes/trial, criterion is exceeded by all of the responses in each distribution, and the point is plotted in the upper right corner of the unit square. As the criterion increases, the number of responses exceeding criterion falls at roughly similar rates for the preferred and null distributions because they are equivalent. The ROC curve therefore falls along the diagonal from the top right of the unit square to the bottom left. For substantially separate response distributions such as those obtained at 25.6 percent correlation, an increasing criterion level exceeds almost all of the null direction responses before exceeding any preferred direction responses. The ROC curve therefore falls near the upper and left-hand boundaries of the unit square. The bend of the ROC curve away from the diagonal is an index of the separation between the preferred and null response histograms.

The expected performance of our decision rule at each correlation level is equal to the area under the corresponding ROC curve. Green and Swets[15] give a formal derivation of this relationship, but one can intuit that it is reasonable. If, for example, we consider the total area of the unit square in Figure 5B to be 1, then the area under the ROC curve for 0.4 percent correlation is 0.535, which represents near chance performance in a two-alternative task (53.5 percent correct). On the other hand, the area under the ROC curve for 25.6 percent correlation is 0.997, indicating that decisions based on the response distributions in the upper panel of Figure 6A will be, as expected, nearly perfect (99.7 percent correct).

We plotted the area under each ROC curve against correlation level to obtain a "neurometric" function such as that illustrated by the open symbols and solid line in Figure 7. This function characterizes the utility of the neuron's responses for discriminating the direction of motion and may be compared directly to the simultaneously observed performance of the monkey (solid circles, dashed line). We fitted a sigmoidal curve to the neurometric function, as described above for the psychometric data, and extracted the parameters indicating threshold and slope of the function. Interestingly, the single MT neuron in Figure 7 was virtually as sensitive to the motion signals as was the monkey: the threshold correlation for the neuron was 6.87 percent as compared to 6.22 percent for the monkey. A comparison of the psychometric and neurometric functions using a likelihood ratio statistic indicated that they were not significantly different ($p > .05$).

Figure 8 shows the relationship between cell threshold and psychophysical threshold for 45 MT neurons from one monkey. Points lying below the diagonal represent neurons whose thresholds are lower than the monkey's. If the monkey could have accurately attended to and counted the impulses from these neurons (and their presumed antineuron partners), his performance would have been better than that actually observed. Points lying above the diagonal indicate neurons that were less sensitive than the monkey's psychophysical performance.

Recall that we tailored the visual stimulus to be optimal for each neuron studied; the aperture size, retinal eccentricity, axis of motion and speed of motion varied from cell to cell. We therefore observed a broad range of psychophysical thresholds during the course of these experiments, ranging from 3 percent to approximately 30 percent correlation. Across this range, the comparison of neuronal and psychophysical data reveals that the sensitivity of MT neurons commonly equaled

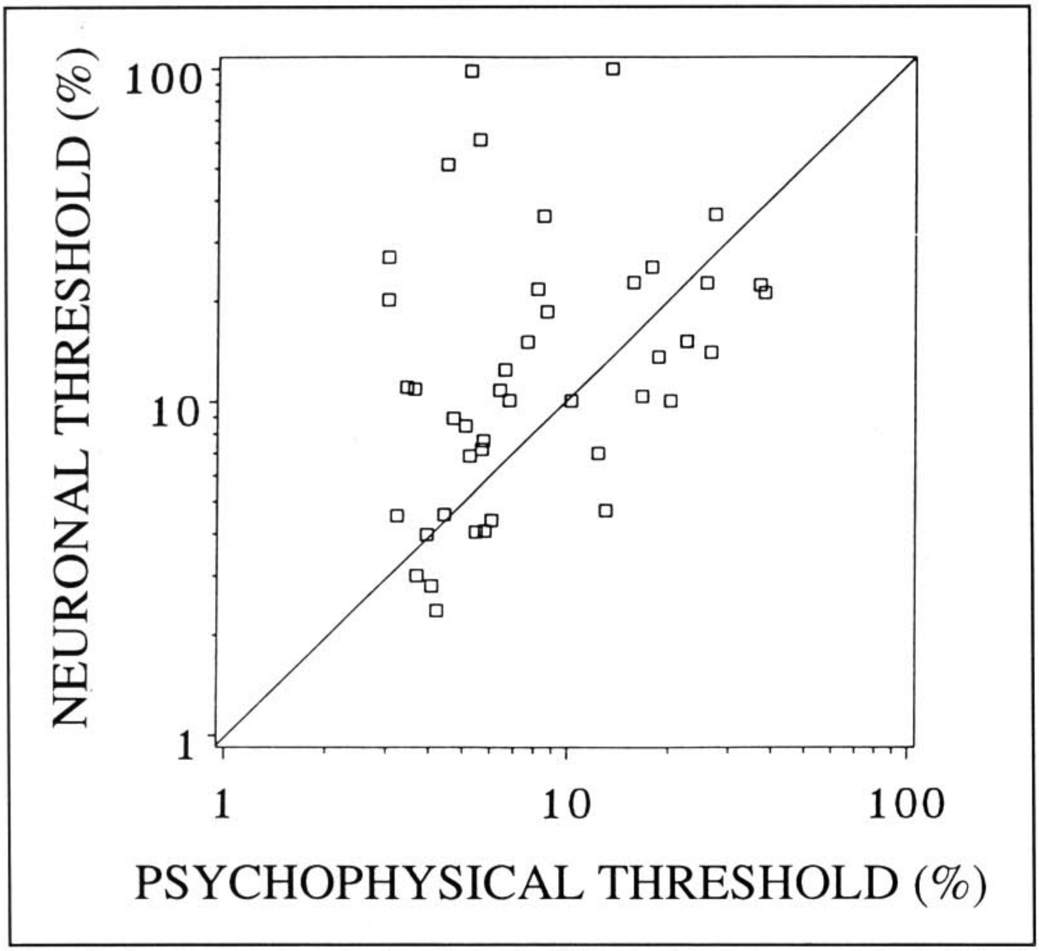

Figure 8. A scatterplot of psychophysical threshold (abscissa) against neuronal threshold (ordinate) for 45 MT neurons studied in one monkey. Points that fall on the diagonal indicate identical thresholds for perception and physiology. For points below the diagonal, neuronal thresholds were lower than psychophysical thresholds; points above the diagonal indicate that psychophysical thresholds were lower. For most MT neurons, cell performance approached or exceeded psychophysical performance.

or exceeded that of the monkey. Neuronal threshold was within a factor of two of psychophysical threshold for 76 percent of the cells, and neuronal threshold was actually lower than psychophysical threshold for 40 percent of the cells. For a minority of cells, neuronal performance was considerably worse than psychophysical performance. Presumably, these cells do not carry signals important for discrimination performance near psychophysical threshold.

Perhaps the most surprising aspect of the data in Figure 8 is that so many cells provide information about stimuli near or below psychophysical threshold. It is natural to wonder why the monkey does not make better use of the information that is clearly present in its cortex. The problem can be explained trivially if the monkey is simply not exerting maximum effort on the discrimination task during the measurements of psychophysical threshold. We believe this to be unlikely because this monkey's psychophysical thresholds were on a par with the best thresholds we have obtained from human observers. In addition, the monkey typically performed at 100 percent correct for suprathreshold stimuli.

A more plausible explanation for the monkey's failure to perform as well as his "best" neurons is uncertainty in the decision process.[17] The reasoning here is that while we, the experimenters, can precisely match the neuron under study with the motion signal activating it, the monkey has no such knowledge. Instead, he is to some degree uncertain about the identity of the stimulus to be discriminated and must therefore base his judgment on the activity of more than just the single neuron under study. Some of these other neurons whose signals contribute may not be well tuned to the particular stimulus, and may therefore contribute a substantial amount of noise that compromises the overall performance of the decision process. This hypothesis predicts that psychophysical performance would be degraded relative to the performance of the "best" neurons.

Pelli[17] used a quantitative model to evaluate the effects of uncertainty on psychophysical decisions. Of particular interest in the present context, he demonstrated that uncertainty would not only make the decision process less sensitive (such as to raise the threshold), but would also steepen the slope of the psychometric function relative to those of the individual analyzers. Figure 9 shows the relationship between neuronal and psychophysical values of β, the slope-related parameter that we extracted while fitting smooth curves to the neurometric and psychometric functions. While there is no correlation between the two measures, the mean value of β for the neurons (1.42) is quite similar to the mean value for psychophysical β, (1.20). Although the estimation of β is rather variable, we conclude that the slopes of the psychometric functions are not systematically elevated in comparison to the slopes of the neurometric functions. This suggests that uncertainty effects in our data are likely to be modest and that the dominant influences on the monkey's decision derive from neurons that are well related to the stimulus. We should recall, however, that there are some neurons whose sensitivity is significantly better than the monkey's, and that some form of uncertainty must therefore contribute to the transformation from neuronal to behavioral performance.

It is well known that pooling of independent signals from individual sources can, in principle, provide more reliable information about near-threshold stimuli than that encoded by any single source.[16,18] If uncertainty effects are small in our paradigm, it is reasonable to inquire why signals are not pooled to permit psychophysical thresholds that are lower than those of individual neurons. A possible reason is that fluctuations in the responses of neurons well tuned to the stimulus are highly correlated, due to the existence of common inputs or mutual excitation. Since the advantage of pooling depends critically on the signals being independent, highly correlated responses would greatly reduce the utility of pooling. Correlated responses among

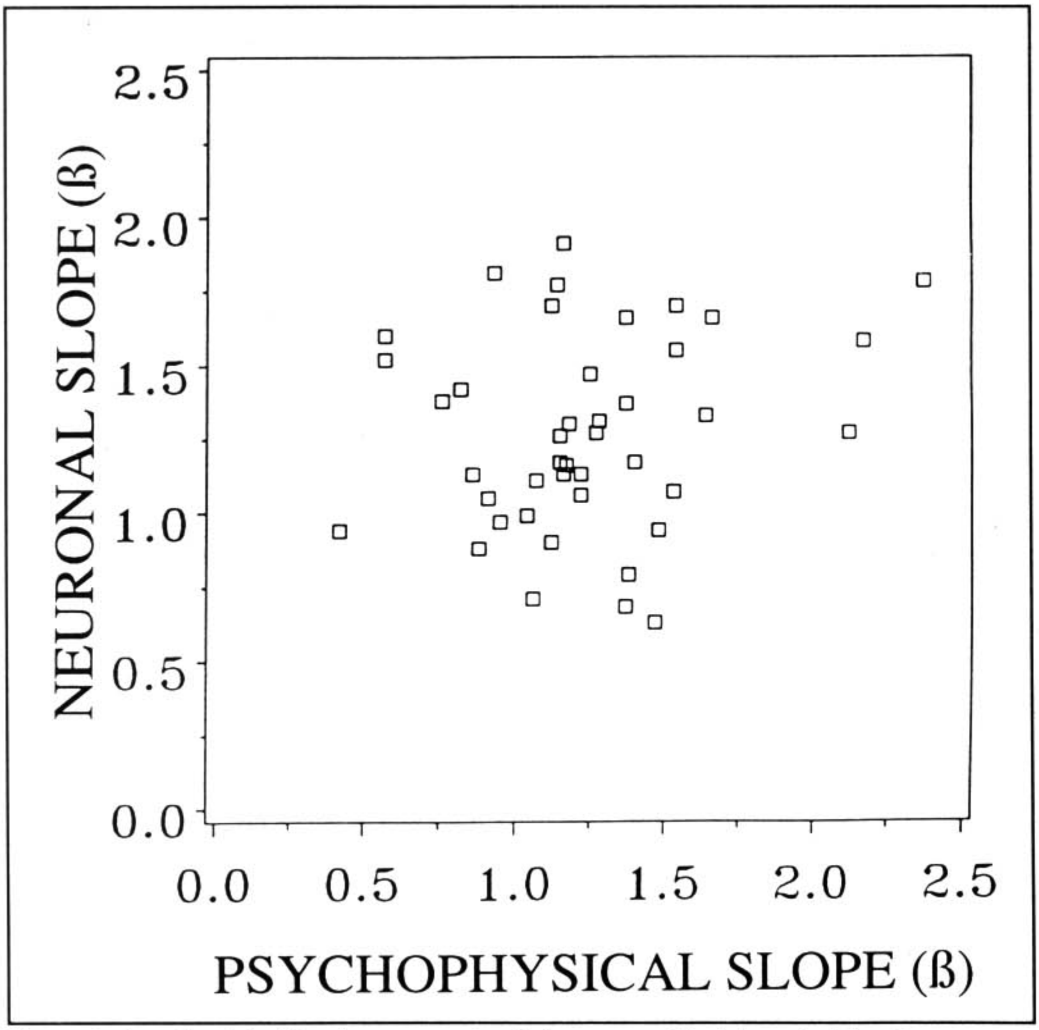

Figure 9. A scatterplot of the slope parameter, β, for neurometric data against the slope parameter for psychometric data. The data were obtained from the same 45 experiments illustrated in Figure 8. There was no systematic correlation between the two slope parameters, but the means of the two distributions were similar (1.42 for the neurometric functions; 1.20 for the psychometric functions).

similarly tuned neurons have been observed in the striate cortex of primates (see Chapter 4 in this volume), and it is reasonable to expect that they are present in MT as well. Whether or not this particular hypothesis is accurate, the similarity of neuronal and psychophysical thresholds indicates that pooling, like uncertainty, is of little consequence for the processing of motion signals in our task.

It appears, then, that perceptual decisions regarding the direction of motion in our visual displays could be based on the responses of MT neurons in a relatively direct manner. Many MT neurons are sufficiently sensitive to the direction of stimulus motion to provide the basis for psychophysical performance near threshold. The lack of strong uncertainty effects suggests that the decisions are not greatly influenced by other neurons that are insensitive to stimulus motion near threshold. In addition, our data indicate that pooling need not be invoked to account for psychophysical performance. We suggest that the perceptual decisions could depend upon a small number of suitably selected cortical neurons.

A Covariation Between Perceptual Decision and Neuronal Response

A psychophysical subject's discrimination of near-threshold stimuli is imperfect. During the threshold measurement illustrated in Figure 3, for example, the monkey identified the direction of motion correctly on 83 percent of the trials at 6.4 percent correlation. Of the 60 trials at 6.4 percent correlation that contained preferred direction motion, the monkey correctly judged motion to be in the preferred direction in 49 trials. In the other 11 trials, he mistakenly indicated that motion was in the null direction. Statistical variation is also present in the responses of MT neurons to repeated presentations of the same stimulus. For example, the hatched histogram in the middle panel of Figure 5A shows that the responses of this neuron varied widely among the 60 trials in which motion was presented in the preferred direction at 6.4 percent correlation. If perceptual decisions made by our task monkey are based on the responses of a small number of MT neurons, it should be possible to detect a trial-by-trial covariation in the strength of the neuron's response and the monkey's decision. In other words, for near-threshold stimuli the monkey may be more likely to select the preferred direction on trials in which the stimulus evokes a relatively large response from the neuron. We have, in fact, observed such an effect in the monkey we have studied most intensively. (A similar effect was reported in alert monkeys trained to detect incremental changes in a noxious thermal stimulus.[19, 20])

Figure 10 illustrates for one MT neuron the responses obtained to stimuli moving in the preferred direction during a psychophysical threshold measurement. The closed symbols depict the mean responses of the neuron in trials in which the monkey correctly decided that motion was in the preferred direction, and the open symbols illustrate responses in trials in which the monkey mistakenly judged motion to be in the null direction. Note that at each correlation level, the same preferred direction stimulus was presented in each trial. The primary difference between the trials represented by the open and closed symbols is the monkey's decision. It is obvious that the monkey decided in favor of the preferred direction in trials in which the neuron, on average, generated a larger response. Interestingly, the effect was present for zero percent correlation trials. Thus even when the monkey was "guessing," he tended to select the preferred direction for trials on which the neuron responded more strongly.

The histograms on the left of Figure 11 show the complete distribution of responses that we observed for three of the correlation levels illustrated in

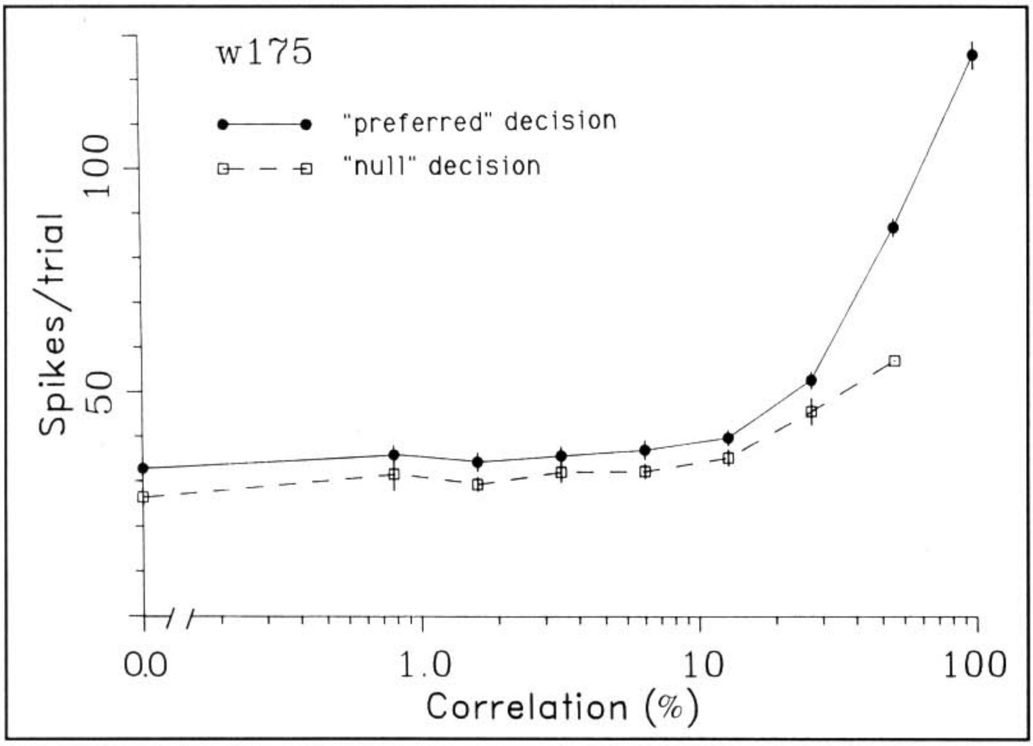

Figure 10. The responses of an MT neuron to motion in the preferred direction at each of several correlation levels. The solid circles and solid line indicate responses on trials in which the monkey correctly judged motion to be in the preferred direction. The open squares and dashed line show responses on trials in which the monkey mistakenly judged motion to be in the null direction. At zero percent correlation, of course, there was no "correct" or "mistaken" judgment, only "preferred" and "null" decisions. Each symbol represents the mean response of the neuron for that condition. 45 trials were presented in the preferred direction at each correlation. The number of incorrect judgements was low for high correlation levels and larger for low correlation levels. The error bars indicate standard error of the means. On the average, decisions in favor of the preferred direction were accompanied by stronger responses from the neuron.

Figure 10. All trials contained motion in the preferred direction; the hatched bars show the response distribution for "preferred" decision trials, and the black bars represent responses for "null" decision trials. We again employed a signal detection analysis to quantify the separation of the two distributions. We generated the family of curves on the right of Figure 11 by the method described above (Figure 5). Again, the curvature away from the diagonal is an index of the separability of the parent distributions. It seems inappropriate, however, to describe these curves as *receiver*-operating characteristics since the parent distributions are not based on differences in the stimuli "received" by the system. Rather, we refer to the curves as *sender*-operating characteristics, or SOC curves, because they are based solely on differences in the output of the system, that is, on the decision made by the monkey. In other words, the information that gives rise to the bend in the SOC curves appears to be related to the signal "sent" by the neuron to the decision process.

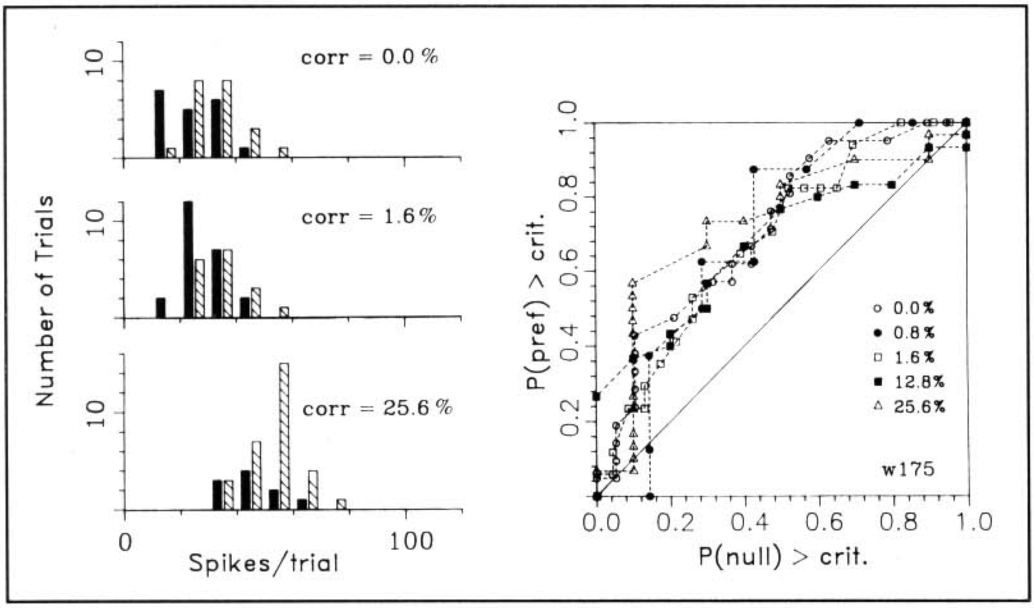

Figure 11. A signal detection analysis of the effect illustrated in Figure 10. **A.** The histograms depict the complete distribution of responses obtained at three correlation levels. Motion occurred in the preferred direction on each trial, with the exception of zero percent correlation trials, which did not contain a correlated motion signal. The hatched bars show the responses of the neuron in trials in which the animal decided in favor of the preferred direction; the solid bars depict responses in trials in which the animal decided in favor of the null direction. For each correlation level, the response distribution for "preferred" decisions is offset to a higher range than the corresponding distribution for "null" decisions. **B.** The right-hand panel of the figure illustrates "sender" operating characteristics (SOC curves) that we computed for five different correlation levels. The SOC curves were computed by the method described previously for ROC curves. The proportion of the unit square lying under an SOC curve represents the probability that an ideal observer could predict the decision of the monkey (preferred or null direction) based only on the response of this neuron. Since we have never seen a systematic relationship between the area under the SOC curve and correlation level, we used a weighted mean of the areas under the family of SOC curves to obtain a single decision-related probability (SOC probability) for each neuron. The contribution of each curve to the weighted mean was proportional to the lesser of the number of errors or correct decisions made by the monkey at that correlation level. For the neuron illustrated in this figure, the decision-related probability was 0.673.

We integrated each SOC curve to obtain a quantitative measure of this effect. For each correlation level, the area under the SOC curve corresponds to the probability that an observer could correctly predict the monkey's perceptual decision based on the response of this neuron. We therefore refer to this metric as a decision-related probability, or SOC probability. Since we have never observed a consistent relation between the decision-related probability and correlation level, we calculated a weighted mean of the areas under the family of SOC curves to obtain a single decision-related probability for each neuron (each SOC curve contributed to the weighted mean in proportion to the lesser of the number of errors or correct decisions made by the monkey at that correlation level). For the neuron whose curves are depicted in Figure 11, the mean decision-related probability for preferred direction stimuli was 0.673.

If there was no covariation between the neuron's response and the monkey's perceptual decision, the SOC curves in Figure 11 would be randomly distributed about the diagonal, and the mean decision-related probability would be near 0.5.

As will be seen below, the decision-related probability for the neuron shown in Figure 11 (0.673), was among the larger values we obtained. To evaluate the reliability with which these values deviated from chance, we used a numerical technique to simulate the expected values that would result from random association between the monkey's response and neuronal activity. After computing the distribution of values expected from these random associations, we established the probability that values as large as those actually observed could have been obtained by chance. For the case presented in Figure 11, this probability was less than 0.01.

We calculated the mean decision-related probability for each of the 45 neurons which we studied in this monkey, and the results are displayed in Figure 12. Figure 12A shows the distribution of probabilities for preferred direction trials. The mean value for all cells was 0.540, and the rightward displacement of the distribution from 0.5 is highly significant (*t*-test, $p < .001$). This indicates that the monkey's tendency to report preferred direction motion in trials that yielded a relatively strong neuronal response is significant for the sample of neurons as a whole.

Though we have considered only preferred direction trials thus far, we carried out the SOC analysis for null direction trials as well. Figure 12B illustrates the results of this analysis. Again, the distribution was significantly displaced to the right of 0.5 (*t*-test, $p < .05$), though the effect was smaller than that for preferred direction trials. Thus a large neuronal response was accompanied, more likely than not, by a decision in favor of the neuron's preferred direction both in trials in which motion occurred in the null direction and in trials that contained motion in the preferred direction. As we indicated previously, the effect is present even for zero percent correlation trials , which do not contain a reliable motion signal. We analyzed these trials independently for each neuron, and Figure 12C shows the distribution of decision-related probabilities across the sample. The distribution is clearly displaced to the right of 0.5 (*t*-test, $p < .001$), confirming the somewhat surprising observation that the monkey's decisions were correlated with the discharge rate of MT neurons even in trials in which the stimulus provided unreliable information concerning direction of motion.

This covariation of neuronal and psychophysical responses suggests that the activity of many MT neurons is intimately related to directional judgments made by the monkey. In our experiments, this relationship was evident near or below threshold, where perceptual judgments are finely balanced between two alternatives. In this situation, the variability of neuronal responses can have a measurable impact on the judgment made by the monkey. The most straightforward interpretation is that these neurons provide the critical signals used by the monkey in

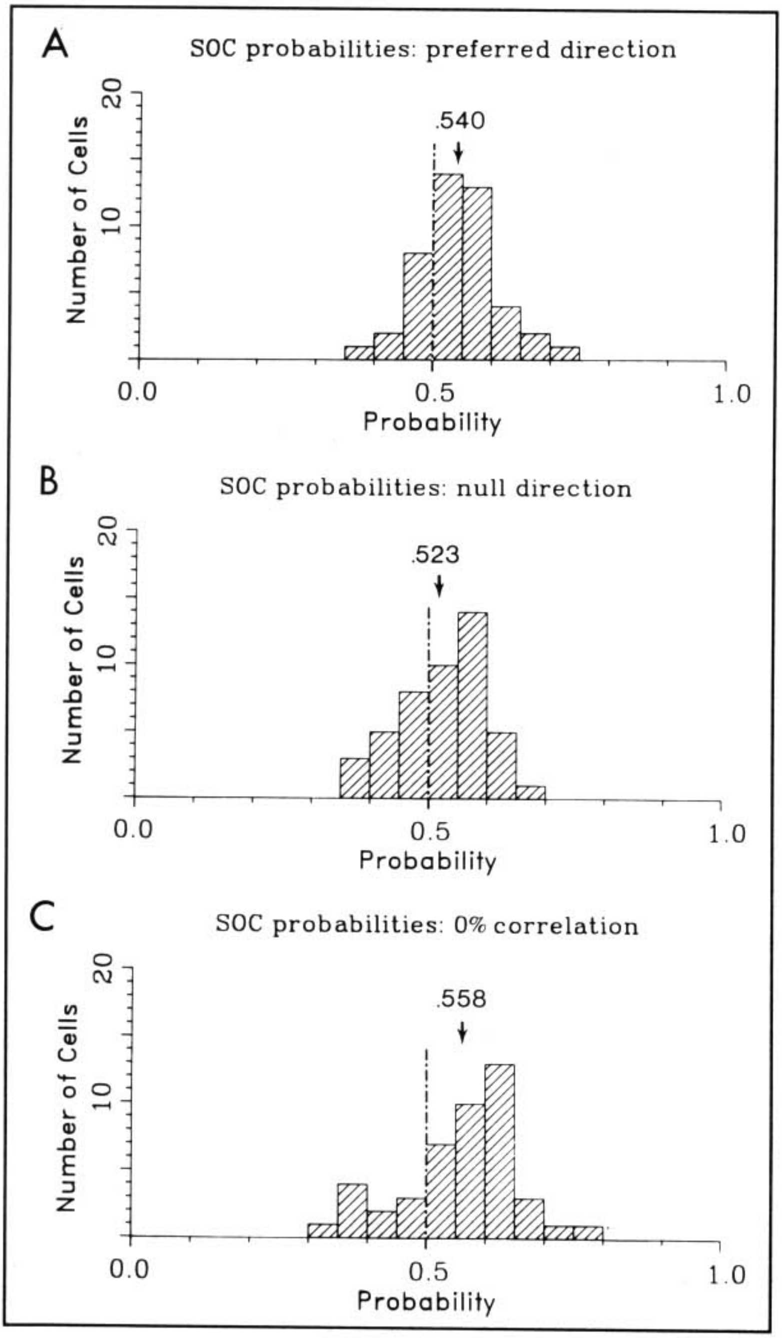

Figure 12. Decision-related probabilities, or SOC probabilities, for 45 neurons in one monkey. **A.** Decision-related probabilities for preferred direction trials. The displacement of the distribution to the right of 0.5 is highly significant (*t*-test, $p < .001$). The arrow indicates the mean of the distribution. **B.** Decision-related probabilities for null direction trials. The rightward displacement of the mean is also significant for null direction trials (*t*-test, $p < .05$) although the effect is smaller (mean = 0.523). **C.** Decision-related probabilities for trials with zero percent correlation only. The rightward displacement of the distribution is highly significant (*t*-test, $p < .001$).

making such directional judgments. That the effect is present for zero percent correlation trials is particularly suggestive: even in the absence of a reliable motion signal, the monkey would appear to base decisions, in part, on the activity of these neurons.

Magnitude of the Decision-Related Probability: Theoretical Considerations

Although the covariation of neuronal and psychophysical responses illustrated in Figures 11 and 12 is significant, it is nevertheless small. The separation in "decision" based distributions such as those illustrated in the histograms of Figure 11 do not approach the best separations for "stimulus" based distributions such as those at the top left of Figure 5. Consequently, the areas under the individual SOC curves are generally much less than one. Interestingly, theoretical consideration of the two-neuron model outlined in Figure 6 indicates that the decision-related probabilities expected from perfect adherence to the model are, like those measured from our neurons, usually less than one. In other words, the experimentally derived probabilities in Figure 12 are closer to the expected values than it might first appear. The logic that leads to this conclusion is developed in Figures 13 and 14.

Consider a hypothetical pair of MT neurons, X and Y, which are selective for rightward and leftward stimulus motion, respectively. For any given stimulus, the responses of X and Y (denoted x and y) would be expected to vary on successive presentations and may be idealized by frequency distributions like those in Figures 13A and 13B. When the stimulus is random motion noise (zero percent correlation) the response distributions of X and Y, $f(x)$ and $f(y)$, are identical, as illustrated in Figure 13A. For a weak rightward-moving stimulus, the response distribution of X is displaced to larger values, as shown in Figure 13B. By the decision rule in Figure 5, directional judgments are made by comparing the responses of the pair of neurons. Motion is judged to be rightward if x exceeds y on a given trial and judged to be leftward if y exceeds x.

If the responses of cells X and Y are independent, then all possible combinations of paired responses from the two cells would be predicted as the product of the two frequency distributions, $f(x)f(y)$. The probability surfaces in Figures 13C and 13D represent the distribution of paired responses for the noise and near-threshold cases, respectively. In both plots, the diagonal line that separates shaded from unshaded regions of the probability surface indicates trials on which equal responses are obtained from the two cells. Trials fall into the unshaded region of the surface if x exceeds y; trials fall into the shaded region if the converse relation obtains. For the zero percent correlation case (noise, Figure 13C), the joint distribution is centered on the diagonal. Thus it is equally likely for either X or Y to yield the larger response. For the threshold case (Figure 13D) the surface is centered to the right of the diagonal and x would be expected to exceed y on the majority of trials.

These relationships may be appreciated in the contour plots in Figures 14A and 14B which represent the same joint probability surfaces as viewed from above. Here the diagonal line clearly distinguishes the portion of the paired response distribution in which x exceeds y from the portion in which y exceeds x. For the zero percent correlation case (14A), the diagonal cuts the contour plot in equal halves, whereas most of the distribution falls below the diagonal ($x > y$) for the threshold stimulus (14B). The decision rule in Figure 6

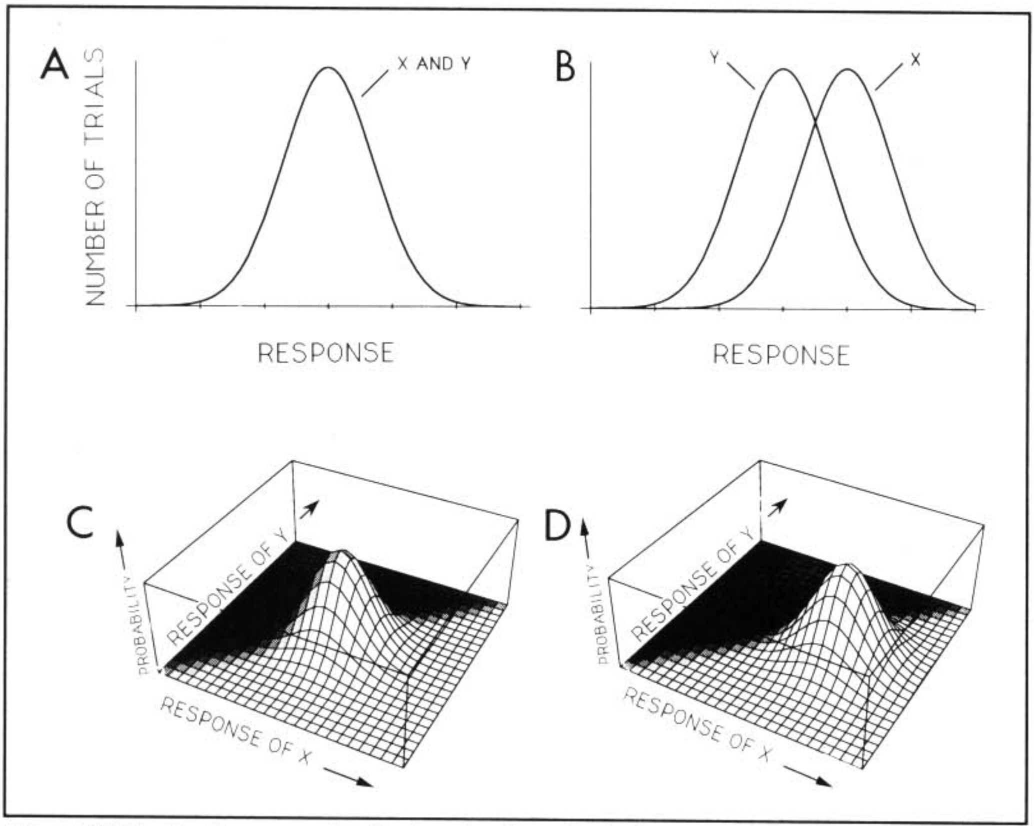

Figure 13. Idealized response distributions for a hypothetical neuron-antineuron pair. As in Figure 6, neuron *X* responds preferentially to rightward motion while "antineuron" *Y* is selective for leftward motion. The response distributions of the two neurons are assumed to be identical except that their preferred directions are reversed. **A.** Response distributions for zero percent correlation (noise) stimuli for neurons *X* and *Y*. Response magnitude is represented on the abscissa in arbitrary units, and the frequency distributions are modeled as Gaussian for purposes of computational convenience (tic marks are separated by $\sqrt{2}$). Since there is no consistent motion in any direction in this stimulus, the distributions are completely overlapping. **B.** The response distributions of *X* and *Y* to rightward motion at a correlation level near psychophysical threshold. Since the neuron, *X*, is selective for rightward motion, its responses are generally larger than those of the antineuron, *Y*. **C.** The joint probability distribution for zero percent correlation trials illustrated in **A**. Displacement on the z-axis reflects the probability of obtaining a particular combination of responses from *X* and *Y* on a single trial. The diagonal at the boundary between the shaded and unshaded regions is the identity line along which the responses of the neuron and anti-neuron are equal. The distribution is symmetrically situated about the diagonal. By the decision rule in Figure 6, trials that fall in the shaded region result in a leftward decision (response of $Y >$ response of X). Similarly, trials that fall in the unshaded region are accompanied by a rightward decision (response of $X >$ response of Y). **D.** The joint probability distribution for the near-threshold correlation value illustrated in **B**. Since the responses of *X* are generally greater than the responses of *Y*, the peak of the joint probability distribution is shifted to the right of the diagonal. Rightward decisions will therefore occur on more trials at this correlation level.

therefore predicts that motion will be judged as rightward for most trials represented in Figure 14B.

We may now derive the expected distribution of responses obtained from cell *X* when motion is judged as rightward, and compare this with the expected distribution of responses when

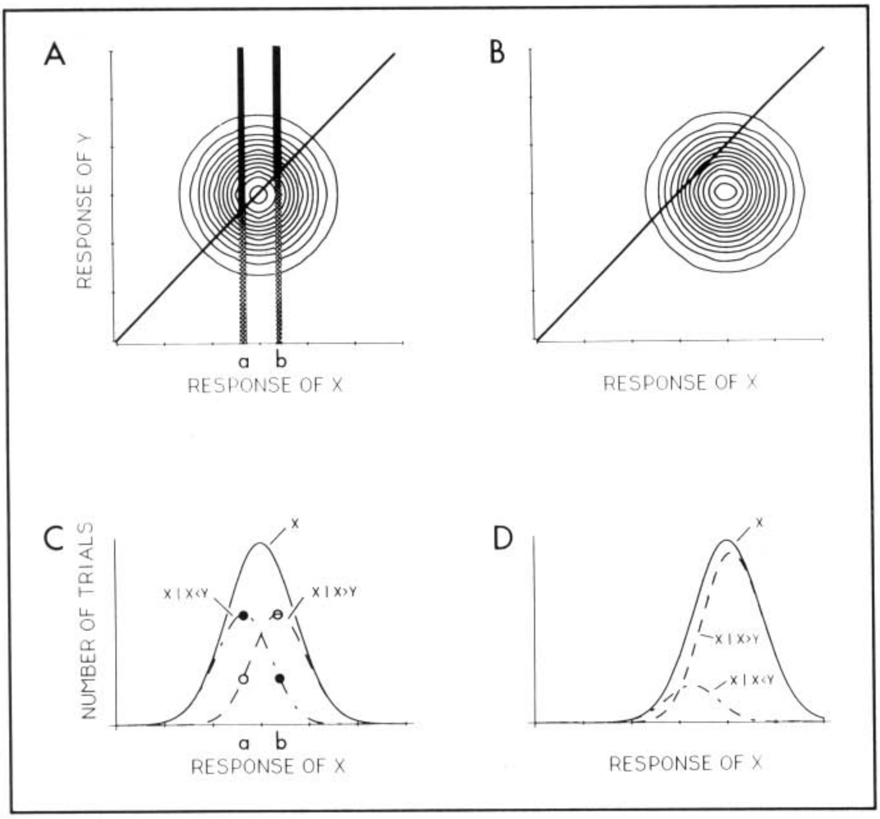

Figure 14. Theoretical prediction of response distributions on rightward and leftward decision trials. **A.** Contour plot representation of the idealized joint response distribution of neuron **X** and "antineuron" **Y** for the zero percent correlation (noise) stimulus. The contours are horizontal slices through the surface shown in Figure 13C. Thus smaller diameter circles indicate higher joint probability. The decision rule is represented by the diagonal line which distinguishes two regions of the distribution. Below the diagonal, trials are represented in which the response of rightward preferring neuron *X* exceeds that of leftward preferring "antineuron" *Y* ($x > y$); above the diagonal the relationship is reversed ($x < y$). Notice that all trials in which neuron *X* responds with strength **a** are described by a slice through the joint distribution at a ($x = \mathbf{a}$). A rightward decision is expected when the response of *Y* is less than **a**, represented by the portion of the slice below the diagonal (stippled). **B.** Contour plot representation of the idealized joint frequency distribution in Figure 13D, representing the paired responses of rightward preferring neuron *X* and leftward preferring "antineuron" *Y* to a weak rightward stimulus. The distribution favors larger responses in *X*. Since most of the distribution falls below the diagonal, rightward decisions are expected on the majority of trials. **C.** Predicted response distributions for neuron *X* on trials in which rightward decisions are made ($x \mid x > y$) and on trials in which leftward decisions are made ($x \mid x < y$) for zero percent correlation (noise) stimuli. These distributions were computed by equations (2) and (3), employing the idealized Gaussian response distributions in Figure 13A. Two examples are shown schematically for a relatively low and high response of neuron *X*, denoted **a** and **b** respectively. Although neuron *X* is equally likely to respond with strength $x = \mathbf{a}$ or $x = \mathbf{b}$, the larger response, **b**, is more likely to be accompanied by a rightward decision. The probability that neuron *X* will respond with magnitude **a** in association with a rightward decision ($y < \mathbf{a}$) is represented by the open circle. This is the area under the joint distribution along the stippled portion of the slice at **a** in the contour plot (panel **A**). The probability that response a will be associated with a leftward decision is shown by the solid circle, reflecting the area under the solid portion of the slice at **a**. The same relations pertain at $x = \mathbf{b}$. The decision-related probability (SOC probability) for these two distributions is 0.83. **D.** The expected response distributions for neuron *X* accompanying rightward decisions ($x \mid x > y$) and leftward decisions ($x \mid x < y$) for a weak rightward moving stimulus. Fewer leftward decisions are predicted and are more likely to be associated with smaller responses of the neuron. The decision-related probability (SOC probability) for these distributions is 0.85.

motion is judged as leftward. Let us consider the zero percent correlation stimulus (Figures. 14A and 14C). The frequency of observing a particular response, **a**, from neuron X is the integral along a slice through the probability surface indicated by the vertical strip at **a** in the contour plot (Figure 14A). The fraction of the integral below the diagonal, indicated by the stippled portion of the slice, reflects the frequency of observing response a when neuron Y yields a smaller response. If the decision rule is obeyed, motion will be judged as rightward on these trials. The fraction of the integral above the diagonal, shown by the solid portion of the slice, reflects the frequency of observing response **a** in neuron X when the response of neuron Y is greater than **a**. For these trials, the decision rule predicts that motion will be judged as leftward. In general, the conditional probability of obtaining any response from neuron X given a *rightward* decision is given by percent

$$f(x|x>y) = f(x)\int_{-\infty}^{x} f(y)dy \qquad (2)$$

where $f(x)$ and $f(y)$ represent the response distributions of neurons X and Y, respectively. Similarly, the conditional probability of obtaining any response from neuron X given a *leftward* decision is given by

$$(x|x<y) = f(x)\int_{x}^{\infty} f(y)dy \qquad (3)$$

Recall that these distributions are estimated from the experimental data: $f(x)$ is the distribution of response values recorded from the neuron under study while the response distribution for the "antineuron," (y), is inferred from the response of the "neuron" to the opposite direction of motion.

Using equations (2) and (3), we computed the expected response distributions for neuron X under the two conditions of interest for the SOC measurement: "leftward" decision and "rightward" decision. Figure 14C shows the result of this computation for a zero percent correlation stimulus, and Figure 14D depicts the result for the weak rightward moving stimulus. In each figure, the expected response distribution for rightward decision trials is given by the dashed line labeled "$x \mid x > y$." Similarly, the expected response distribution for leftward decision trials is indicated by the dashed line labeled "$x \mid x < y$." Of course, the sum of the dashed curves in each figure must equal the original distribution of responses for neuron X shown in Figures 13A and 13B and indicated again by the solid curves in Figures 14C and 14D.

An intuitive feel for the predicted distributions may be gained by considering the vertical "integration strips" at points **a** and **b** in Figure 14A. Integration along the stippled portion of the strip at **a** will yield a smaller value than integration along the solid portion because more of the joint probability surface lies above the diagonal at **a**. Thus the probability of obtaining response **a** from neuron X will be smaller for the condition $x > y$ (rightward decision) than for the condition $x < y$ (leftward decision). The expected frequencies for the two conditions are indicated by the open circle (on the curve $x > y$)

and the closed circle (on the curve $x < y$) at point **a** in Figure 14C. The opposite relation obtains for the strip at point **b** in Figure 14A. Integration along the stippled portion of this strip yields a larger value than integration along the solid portion since more of the joint probability surface lies below the diagonal at this point. Thus, the likelihood of obtaining response **b** is greater for trials in which rightward decisions are made (open circle at **b** in Figure 14C) than for trials on which leftward decisions are made (closed circle).

We may now compare the theoretically derived distributions in Figures 14C and 14D with experimentally observed distributions such as those illustrated on the left of Figure 11. Although the experimental distributions in Figure 11 appear rather rough due to the modest number of trials recorded at each correlation level, they are qualitatively similar to the theoretical results. For the zero percent correlation case (Figure 14C; top left of Figure 11), the distribution for "preferred" decision trials overlaps, but is offset to the right of, the distribution for "null" decision trials in both the theoretical and experimental data. For the near-threshold case (Figure 14D; lower left of Figure 11), the theoretical and experimental data both yield a striking difference in amplitude between the distributions for "preferred" and "null" decisions. This is a natural consequence of the fact that a larger proportion of correct decisions occurs near threshold than at zero percent correlation. More importantly, the offset and overlap of the distributions for "preferred" and "null" decisions are again similar for the theoretical and experimental data. Qualitatively, then, the observed distributions for the MT neuron in Figure 11 conform to the results expected from the two-neuron model.

It is possible to evaluate quantitatively the correspondence between theory and experiment by comparing the decision-related probabilities for the idealized distributions in Figures 14C and D with those obtained for the MT neuron in Figure 11. For the theoretical distributions, the probability was 0.83 for the zero percent correlation case (Figure 14C) and 0.85 for the near-threshold case (Figure 14D). Thus the decision-related probabilities expected from perfect adherence to the two-neuron decision rule, like those of our neurons, are substantially less than one. For the experimental data, the corresponding probabilities were 0.71 (zero percent correlation) and 0.73 (25.6 percent correlation). While the theoretical and experimental data are qualitatively similar, then, the decision-related probabilities for this MT neuron fall somewhat short of the expected values. Recalling that the neuron in Figure 11 yielded one of the largest decision-related probabilities in our sample of cells, we would expect this quantitative discrepancy between theory and experiment to be generally true in our data. A preliminary analysis has shown this to be the case.

The most likely explanation for the discrepancy is that the basic assumptions of the two-neuron model are overly simplistic. In other words, there is more variance in the monkey's decisions than can be accounted for by a comparison of only two oppositely tuned neurons. This is hardly surprising; even the most ardent single-unit physiologist would concede that perceptual decisions in our task are likely to depend upon a somewhat larger collection of neurons, perhaps comprising the most sensitive neurons in a few cortical columns. What is remarkable about the comparison between theory and experiment is that the decision-related probabilities from single MT neurons can approach as closely as they do to those predicted by the two-neuron model. This observation lends additional support to our hypothesis that perceptual decisions in this task are based on the responses of a small number of neurons.

We have argued that the covariation in neuronal response and psychophysical response revealed by the SOC analysis arises because the monkey's perceptual decisions are based on the directional signals encoded by MT neurons. However, alternative explanations must be considered. For example, the covariation may result from a third variable, such as attention, which is not under adequate experimental control. One might suppose that increased attention in a particular trial has the effect of enhancing slightly the responsiveness of neurons across a large portion of the visual cortex. If increased attention also elevated the probability of the monkey making a correct decision, then a correlation between increased neuronal responsiveness and correct decisions would be expected in the absence of a causal relationship between the two. However, the attention hypothesis cannot explain the covariation of neuronal response and psychophysical decision on zero percent correlation trials. For these trials there are no "correct" or "incorrect" decisions since there is no net motion in the stimulus. There are only "preferred" and "null" direction responses.

Whatever variable is postulated to explain the effect must occur only in trials in which the monkey emits a "preferred" response. The most obvious event that occurs only in "preferred" decision trials is the operant response itself, the eye movement to the preferred target. However, we have never observed saccade-related activity in MT, and lesions of this area have no effect on saccades to stationary targets.[21] In addition, the changing geometry of receptive-field location and preferred-null axis for individual MT neurons ensures that no particular metric of the saccade will be associated consistently with the target LED for a preferred-direction choice. We are therefore skeptical that the eye movement itself could account for the covariation between neuronal response and psychophysical decision.

Finally, we should point out that inter-animal variability in the selectivity of inputs to the monkey's decision process could yield different patterns of results in different animals. All the data we have presented were obtained in a single monkey, and the data suggest that the directional judgments made by this animal were based in a selective manner on neurons that are well tuned for, and highly sensitive to, the motion signals in our visual displays. If the decisions made by another animal were more strongly influenced by the activity of neurons that are poorly related to the stimulus, our experiments could reveal a wider gap between sensitivity of the "best" neurons and psychophysical sensitivity (see discussion of uncertainty effects in a preceding section) as well as a diminution or absence of the covariation of neuronal response and psychophysical decision. We have obtained preliminary data from a second monkey in which both of these trends are evident, but a reliable indication of the inter-animal variability in these results must await more extensive data from a larger pool of animals.

Conclusions

Earlier in this chapter, we suggested that a physiological understanding of a perceptual process would include: (1) identification of the neurons that provide the critical signals for the perceptual decision, (2) insight into the way these signals arise from the inputs provided by lower visual centers, and (3) knowledge of the mechanisms by which the critical signals are translated into a decision. Although preliminary, our results are relevant to these issues and suggest experiments that will further clarify the physiological basis of the perceptual decisions made by the monkey in our task.

Previous experiments which combined psychophysical testing with cortical lesions indicated that MT is necessary for normal performance on the psychophysical task employed in the current study.[5] Our ROC analysis of the physiological data obtained during performance of this task shows that the directional information encoded by single MT neurons is often sufficient to account for psychophysical performance. Considered together, these findings suggest that the directional signals encoded by MT neurons contribute to the monkey's perceptual decision.

This point of view is strengthened considerably by the observation of a trial-by-trial association between the intensity of response of an MT neuron and the likelihood that the monkey would judge motion to be in the neuron's preferred direction. Thus some MT neurons contain information about the decision that the monkey will make in a trial, independent of the stimulus presented to the system. Although additional data are needed to interpret this effect conclusively, the covariation of neuronal response and perceptual decision provides evidence for a relatively direct link between MT and the monkey's decision process.

It will be of interest to determine how the sensitivity of MT neurons to motion is related to that of antecedent neurons in the central visual pathway (point 2 above). It is clear, for example, that many directionally selective neurons in striate cortex (V1) project to MT,[22] and anatomical experiments have shown that MT receives inputs from V2 and V3 as well.[23,24] We suspect that neurons in these areas will not exhibit the striking correspondences between neuronal and psychophysical performance for the stimuli employed in the present study. If, however, the stimuli are modified to be optimal for neurons in V1, V2 and V3 (smaller apertures, slower speeds, higher dot densities), correspondences between neuronal and psychophysical performance may emerge. We will address issues of this nature in future experiments.

The present data are also relevant to the third, and most difficult, point raised above: the mechanisms by which sensory signals are translated into perceptual decisions. Our theoretical consideration of the sender-operating characteristic indicates that a decision rule based on a comparison of the responses of neurons with opposite preferred directions can account qualitatively for the covariation between neuronal response and perceptual decision. This finding provides physiological support for the notion, based initially on psychophysical evidence, that perceptual judgments concerning direction of motion result from a comparison of oppositely tuned directional mechanisms. Exactly where and how this comparison is made remains to be determined. Our data are consistent with the idea that MT neurons provide relatively direct inputs to the mechanism that implements the comparison, and we plan to search for neuronal correlates of this mechanism in the higher cortical areas that receive projections from MT.

In principle, the output of the comparison mechanism should be a signal that reflects the animal's decision more directly. Clearly, such signals exist in oculomotor centers such as the superior colliculus since the monkey must decide on a given trial whether to move its eyes to one or the other target. Our goal, however, is to trace more accurately the transition from sensory signals to decision-related signals by recording at intermediate levels of the pathway. The fact that we can observe both sorts of signals in the activity of MT neurons suggests that the transition may be graded, with sensory responses gradually giving way to decision-related responses. Additional insight into the nature of this transition should come about from continued analysis of these signals in the cortex of behaving monkeys.

Acknowledgments

We are grateful to Drs. Stanley Klein, Laurence Maloney, Denis Pelli and Brian Wandell for insightful comments and suggestions at various stages of this project. The work was supported by grants from the National Eye Institute (EY 5603 and EY 2017), and by a McKnight Development Award to W.T.N.

References

1. D.C. Van Essen, in *Cerebral Cortex, Vol. 3*, A. Peters and E.G. Jones, Eds. (Plenum, New York, 1985), pp. 259-329.
2. J.H.R. Maunsell and W.T. Newsome, in *Annual Review of Neuroscience, Vol. 10*, M. Cowan, E. Shooter, C. Stevens, and R. Thompson, Eds. (Annual Reviews Inc., Palo Alto, 1987), pp. 363-402.
3. T. Pasternak *et al., Exp. Brain Res.* **61,** 214 (1985).
4. T. Pasternak and L. Leinen, *J. Neurosci.* **6,** 938 (1986).
5. W.T. Newsome and E.B. Paré, *J. Neurosci.* **8,** 2201 (1988) .
6. J.A. Movshon *et al.*, in *Pattern Recognition Mechanisms*, C. Chagas, R. Gattass, and C. Gross, Eds. (Springer-Verlag, New York, 1986), pp. 117-151.
7. S.M. Zeki, *J. Physiol.* **236,** 549 (1974).

8. J.F. Baker *et al., J. Neurophysiol.* **45,** 397 (1981).

9. J.H.R. Maunsell and D.C. Van Essen, *J. Neurophysiol.* **49,** 1127 (1983).

10. T.D. Albright, *J. Neurophysiol.* **52,** 1106 (1984)

11. A.B. Watson, *Vision Res.* **19,** 515 (1979).

12. R.F. Quick, *Kybernetik* **16,** 65 (1974).

13. R. Sekuler, A. Pantle, and E. Levinson, in *Handbook of Sensory Physiology, Vol. 8,* H.L. Teuber, Ed. (Springer-Verlag, Berlin, 1978), pp. 67-96.

14. S. Anstis, in *Handbook of Perception and Human Performance, Vol. 1,* K.R. Boff, L. Kaufman, and J. P. Thomas, Eds. (John Wiley and Sons, New York, 1986), pp. 16-1 to 16-27.

15. D.M. Green and J.A. Swets, *Signal Detection Theory and Psychophysics* (Wiley, New York, 1966).

16. D.J. Tolhurst, J.A. Movshon, and A. F. Dean, *Vision Res.* **23,** 775 (1983).

17. D.G. Pelli, *J. Opt. Soc. Am.* **A 2,** 1508 (1985).

18. M.H. Pirenne, *Nature (London)* **152,** 698 (1943).

19. W. Maixner *et al., Brain Res.* **374,** 385 (1986).

20. D.R. Kenshalo *et al., Brain Res.* **454,** 378 (1988).

21. W.T. Newsome *et al., J. Neurosci.* **5,** 825 (1985).

22. J.A. Movshon and W.T. Newsome, *Soc. Neurosci. Abst.* **10,** 933 (1984).

23. J.H.R. Maunsell and D.C. Van Essen, *J. Neurosci.* **3,** 2563 (1983).

24. L.G. Ungerleider and R. Desimone, *J. Comp. Neurol.* **248,** 190 (1986).

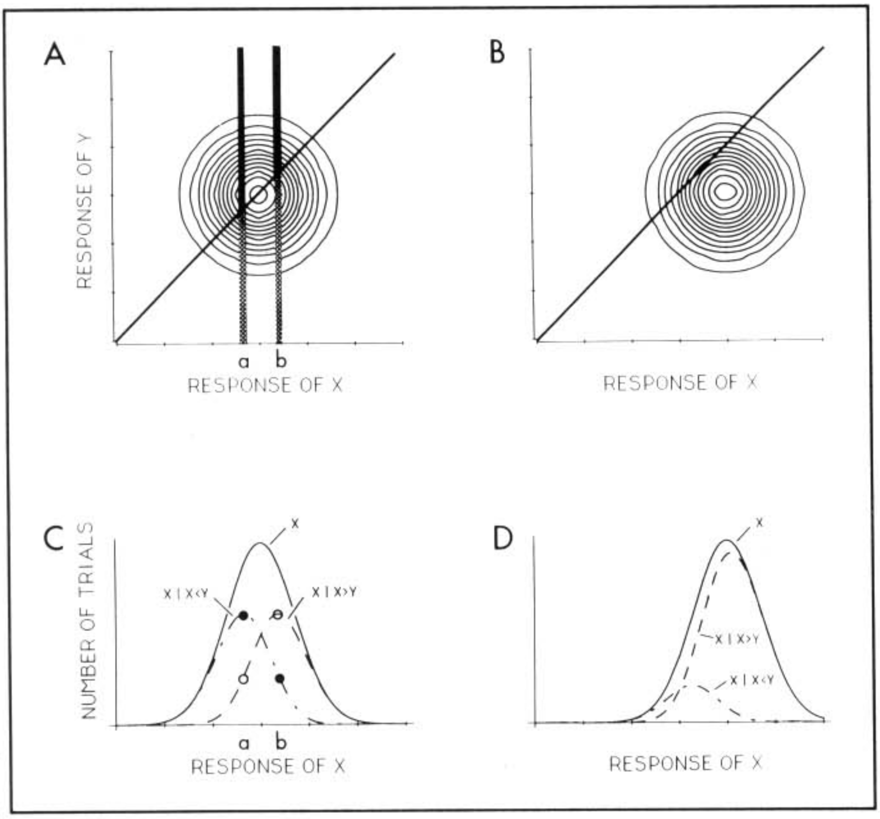

Figure 14. Theoretical prediction of response distributions on rightward and leftward decision trials. **A.** Contour plot representation of the idealized joint response distribution of neuron **X** and "antineuron" **Y** for the zero percent correlation (noise) stimulus. The contours are horizontal slices through the surface shown in Figure 13C. Thus smaller diameter circles indicate higher joint probability. The decision rule is represented by the diagonal line which distinguishes two regions of the distribution. Below the diagonal, trials are represented in which the response of rightward preferring neuron *X* exceeds that of leftward preferring "antineuron" *Y* $(x > y)$; above the diagonal the relationship is reversed $(x < y)$. Notice that all trials in which neuron *X* responds with strength **a** are described by a slice through the joint distribution at a $(x = \boldsymbol{a})$. A rightward decision is expected when the response of *Y* is less than **a**, represented by the portion of the slice below the diagonal (stippled). **B.** Contour plot representation of the idealized joint frequency distribution in Figure 13D, representing the paired responses of rightward preferring neuron *X* and leftward preferring "antineuron" *Y* to a weak rightward stimulus. The distribution favors larger responses in *X*. Since most of the distribution falls below the diagonal, rightward decisions are expected on the majority of trials. **C.** Predicted response distributions for neuron *X* on trials in which rightward decisions are made $(x \mid x > y)$ and on trials in which leftward decisions are made $(x \mid x < y)$ for zero percent correlation (noise) stimuli. These distributions were computed by equations (2) and (3), employing the idealized Gaussian response distributions in Figure 13A. Two examples are shown schematically for a relatively low and high response of neuron *X*, denoted **a** and **b** respectively. Although neuron *X* is equally likely to respond with strength $x =$ **a** or $x =$ **b**, the larger response, **b**, is more likely to be accompanied by a rightward decision. The probability that neuron *X* will respond with magnitude **a** in association with a rightward decision $(y <$ **a**$)$ is represented by the open circle. This is the area under the joint distribution along the stippled portion of the slice at **a** in the contour plot (panel **A**). The probability that response a will be associated with a leftward decision is shown by the solid circle, reflecting the area under the solid portion of the slice at **a**. The same relations pertain at $x =$ **b**. The decision-related probability (SOC probability) for these two distributions is 0.83. **D.** The expected response distributions for neuron *X* accompanying rightward decisions $(x \mid x > y)$ and leftward decisions $(x \mid x < y)$ for a weak rightward moving stimulus. Fewer leftward decisions are predicted and are more likely to be associated with smaller responses of the neuron. The decision-related probability (SOC probability) for these distributions is 0.85.